

# Backdoor Attacks on Discrete Graph Diffusion Models

Jiawen Wang  
Illinois Institute of Technology  
jwang306@hawk.iit.edu

Yuan Hong  
University of Connecticut  
yuan.hong@uconn.edu

Samin Karim  
Illinois Institute of Technology  
skarim7@hawk.iit.edu

Binghui Wang  
Illinois Institute of Technology  
bwang70@iit.edu

## Abstract

Diffusion models are powerful generative models in continuous data domains such as image and video data. Discrete graph diffusion models (DGDMs) have recently extended them for graph generation, which are crucial in fields like molecule and protein modeling, and obtained the SOTA performance. However, it is risky to deploy DGDMs for safety-critical applications (e.g., drug discovery) without understanding their security vulnerabilities.

In this work, we perform the first study on graph diffusion models against backdoor attacks, a severe attack that manipulates both the training and inference/generation phases in graph diffusion models. We first define the threat model, under which we design the attack such that the backdoored graph diffusion model can generate 1) high-quality graphs without backdoor activation, 2) effective, stealthy, and persistent backdoored graphs with backdoor activation, and 3) graphs that are permutation invariant and exchangeable—two core properties in graph generative models. 1) and 2) are validated via empirical evaluations without and with backdoor defenses, while 3) is validated via theoretical results<sup>1</sup>.

## 1 Introduction

Diffusion models have recently driven transformative advancements in generative modeling across diverse fields: image generation [38, 11, 8], audio generation [18, 25], video generation [12]. Inspired by nonequilibrium thermodynamics [38], these models employ a unique two-stage approach involving forward and reverse diffusion processes. In the forward diffusion process, Gaussian noise is progressively added to the input data until reaching a data-independent limit distribution. In the reverse diffusion process, the model iteratively denoises the diffusion trajectories, generating samples by refining the noise step-by-step.

This success of diffusion models for *continuous* data brings new potentials for tackling graph generation, a fundamental problem in various applications such as drug discovery [23] and molecular and protein design [26, 24, 10]. The first type of approach [34, 15, 52] adapts diffusion models for graphs by embedding them in a *continuous space* and adding Gaussian noise to node features and adjacency matrix. However, this process produces complete noisy graphs where the structural properties like sparsity and connectivity are disrupted, hindering the reverse denoising network

<sup>1</sup>Source code is available at: <https://github.com/JiawenWang1104/BA-DGDM>

to effectively learn the underlying structural characteristics of graph data. To address the limitation, the second type of approach [39, 17, 4, 22, 10, 54, 51] proposes *discrete* graph diffusion model (DGDM) tailored to graph data. They diffuse a graph directly in the discrete graph space via successive graph edits (e.g., edge insertion and deletion). Especially, the recent DGDMs [39, 51] can preserve the marginal distribution of node and edge types during forward diffusion and the sparsity in intermediate generated noisy graphs (more details see Section 3). In this paper, we focus on DGDMs, as they have also obtained the state-of-the-art performance on a wide range of graph generation tasks, such as the small and large molecule generation.

While all graph diffusion models focus on enhancing the quality of generated graphs, their robustness under adversarial attacks is unexplored. Adopting graph diffusion models for safety-critical tasks (e.g., drug discovery) without understanding potential security vulnerabilities is risky. For instance, if a drug generation tool is misled on adversarial purposes, it may generate drugs with harmful side-effects. We take the first step to study the robustness of DGDMs [39, 51] against backdoor attacks. We note that several prior works [58, 48, 53] show graph *classification* models are vulnerable to backdoor attacks. In this setting, an attacker injects a *subgraph* backdoor trigger into some training graphs and alters their labels as the attacker-chosen target label. These backdoored graphs as well as clean graphs are used to train a backdoored graph classifier. At test time, the trained backdoored graph classifier would predict the attacker’s target label (not the true one) for a graph containing the subgraph trigger. *However, generalizing these attack ideas for our purpose is insufficient*: backdoor attacks on graph classifiers simply alter the training graphs and their labels to implant backdoors, while on graph diffusion models require complex alterations to not only the training graphs, but also the underlying forward and reverse diffusion processes.

**Our work:** We aim to design a backdoor attack by utilizing the unique properties of discrete noise diffusion and denoising within training and generation in DGDMs. At a high-level, the backdoored DGDM should satisfy below goals:

1. *Utility preservation*: The backdoored DGDM should minimally affect the quality of the generated graphs without activating the backdoor trigger.
2. *Backdoor effectiveness, stealthiness, and persistence*: The backdoored DGDM should generate expected backdoored graphs when the trigger is activated. Moreover, the backdoor should be stealthy and persistent, meaning not easy to be detected/removed via backdoor defenses.
3. *Permutation invariance*: Graphs are invariant to the node reorderings. This requires the learnt backdoored model should not change outputs with node permutations.
4. *Exchangeability*: All permutations of generated graphs should be equally likely [16, 50]. In other words, the generated graph distribution is exchangeable.

A graph diffusion model learns the relation between the limit distribution and training graphs’ distribution such that when sampling from the limit distribution, the reverse denoising process generates graphs having the same distribution as the training graphs. We are motivated by this and design the attack on DGDMs to ensure: i) backdoored graphs and clean graphs produce different limit distributions under the forward diffusion process; and ii) the relations between backdoored/clean graphs and the respective backdoored/clean limit distribution are learnt after the backdoored DGDM is trained. Specifically, we use *subgraph* as a backdoor trigger, following backdoor attacks on graph classification models [58, 48, 53]. We then use the forward diffusion process in DGDMs for clean graphs, and *carefully design the forward diffusion process for backdoored graphs (i.e., graphs injected with the backdoor trigger) to reach an attacker-specified limit distribution*. To

ensure a stealthy and persistent attack, we use a small trigger and guarantee it is kept in the whole forward process. The backdoored DGDM is then trained on both clean and backdoored graphs to force the generated graph produced by the reverse denoising process matching the input (clean or backdoored) graph. We also prove our backdoored DGDM is node permutation invariant and generates exchangeable graph distributions.

Our contributions can be summarized as follows.

- We are the first work to study the robustness of graph diffusion models under graph backdoor attacks. We clearly define the threat model and design the attack solution.
- We prove our backdoored graph diffusion model is *permutation invariant* and generates *exchangeable* graphs—two key properties in graph generative models.
- Evaluations on multiple molecule datasets show our attack marginally affects clean graph generation, and generates the stealthy and persistent backdoor, that is hard to be identified or removed with current backdoor defenses.

## 2 Related Work

**Graph generative models:** We classify them as *non-diffusion* and *diffusion* based methods.

**1) Non-diffusion graph generative models:** These methods are classified as *non-autoregressive* and *autoregressive* graph generative models. Non-autoregressive models generate all edges *at once*, and utilize variational autoencoder (VAE) [37, 29, 26, 56], generative adversarial network (GAN) [32], and normalizing flow (NF) [30, 57, 19] techniques. VAE- and GAN-based methods generate graph edges independently from latent representations, but they face limitations in the size of produced graphs. In contrast, NF-based methods require invertible model architectures to establish a normalized probability distribution, which can introduce complexity and constrain model flexibility.

Autoregressive models build graphs by adding nodes and edges sequentially, using frameworks like NF [36, 27], VAE [13, 14], and recurrent networks [23, 55, 7]. These methods are effective at capturing complex structural patterns and can incorporate constraints during generation, making them superior to non-autoregressive models. However, a notable drawback is their sensitivity to node orderings, which affects training stability and generation performance [17, 39].

**2) Graph diffusion models:** Initial attempts for graph generation follow diffusion models that rely on continuous Gaussian noise [34, 15, 52]. However, continuous noises have no meaningful interpretations for graph data [24]. To address it, many approach [39, 17, 4, 24, 22, 10, 54, 51] propose *discrete* diffusion model tailored to graph data. For instance, DiGress [39] extends [24] to tailor graph generation with categorical node and edge attributes. By preserving sparsity and structural properties of graphs through a discrete noise model, DiGress effectively captures complex relationships within graphs, particularly crucial for applications like drug discovery and molecule generation, and obtains the SOTA performance. DiGress is also permutation invariant, produces large graphs, and generated graphs are unique and valid, thanks to the exchangeable distribution.

**Backdoor attacks on graph classification models:** Various works [60, 6, 41, 28, 33, 43, 45, 44] have shown that graph classification models are vulnerable to *inference-time* adversarial attacks. [58] designs the first training- and inference-time backdoor attack on graph *classification* models. It injects a *random subgraph* (e.g., via the Erdős–Rényi model) trigger into some training graphs at random nodes and change graph labels to the attacker’s choice. [48] optimizes the subgraph trigger in

order to insert at vulnerable nodes. Instead of using random subgraphs, [59] embeds carefully-crafted *motifs* as backdoor triggers. Lately, [53] generalizes backdoor attacks from centralized to federated graph classification and shows more serious security vulnerabilities in the federated setting. In addition, these works [58, 53, 9] show existing defenses based on backdoor detection or removal are ineffective against adaptive/strong backdoor attacks.

**Backdoor attacks on non-graph diffusion models:** Two recent work [3] [5] concurrently show image diffusion models are vulnerable to backdoor attacks, where the backdoor trigger is a predefined image object. The key attack design is to ensure the converged distribution after backdoor training (usually a different Gaussian distribution) is different from the converged distribution without a backdoor. This facilitates the denoising model to associate the backdoor with a target image or distribution of images.

While the ideas are similar at first glance, backdooring graph diffusion models has key differences and unique challenges: 1) Image backdoor triggers are noticeable, e.g., an eyeglass or a stop sign is used as a trigger in [5], which can be detected or filtered via statistical analysis on image features. Instead, our subgraph trigger is stealthy (see Table 5). 2) The backdoored forward process in image diffusion models can be easily realized via one-time trigger injection; Such a strategy is ineffective to backdoor graph diffusion models as shown in Table 4. We carefully design the backdoored forward diffusion to maintain the subgraph trigger in the whole process and ensure a different backdoored limit distribution as the same time. 3) Uniquely, backdoored graph diffusion models needs to be node permutation invariant and generate exchangeable graphs.

### 3 Background

#### 3.1 Diffusion Model

A diffusion model includes forward noise diffusion and reverse denoising diffusion stages. Given an input  $z$ , the forward noise diffusion model  $q$  progressively adds a noise to  $z$  to create a sequence of increasingly noisy data points  $(z^1, \dots, z^T)$ . The forward progress has a Markov structure, where  $q(z^1, \dots, z^T|z) = q(z^1|z) \prod_{t=2}^T q(z^t|z^{t-1})$ . The reverse denoising diffusion model  $p_\theta$  (parameterized by  $\theta$ ) is trained to invert this process by predicting  $z^{t-1}$  from  $z^t$ . In general, a diffusion model satisfies below properties:

- **P1:** The distribution  $q(z^t|z)$  has a closed-form formula, to allow for parallel training on different time steps.
- **P2:** The limit distribution  $q_\infty = \lim_{T \rightarrow \infty} q(z^T)$  does not depend on  $x$ , so used as a prior distribution for inference.
- **P3:** The posterior  $p_\theta(z^{t-1}|z^t) = \int q(z^{t-1}|z^t, z) dp_\theta(x)$  should have a closed-form expression, so that  $x$  can be used as the target of the neural network.

#### 3.2 Discrete Graph Diffusion Model: DiGress

We review DiGress [39], the most popular DGDM<sup>2</sup>. DiGress handles graphs with categorical node and edge attributes. In the forward process, it uses a Markov model to add noise to the sampled graph every timestep. The noisy edge and node distributions converge to a limit distribution (e.g.,

---

<sup>2</sup>The latest DGDM DisCo [51] shares many properties with DiGress, e.g., use Markov model, same backbone architecture, converge to marginal distribution over edge and node types, and node permutation invariant.

marginal distribution over edge and node types). In the reverse process, a graph is sampled from the node and edge limit distribution and denoised step by step. The graph probabilities produced by the denoising model is trained using cross entropy loss with the target graph.

Let a graph be  $G = (X, E) \in \mathcal{G}$  with  $n$  nodes,  $a$  node types  $\mathcal{X}$ , and  $d$  edge types  $\mathcal{E}$  (absence of edge as a particular edge type), and  $\mathcal{G}$  the graph space.  $x_i$  denotes node  $i$ 's attribute,  $x_i \in \mathbb{R}^a$  its one-hot encoding, and  $X \in \mathbb{R}^{n \times a}$  all nodes' encodings. Likewise, a tensor  $E \in \mathbb{R}^{n \times n \times d}$  groups the one-hot encodings  $\{e_{ij}\}$  of all edges  $\{e_{ij}\}$ .

**Forward noise diffusion:** For any edge  $e$  (resp. node), the transition probability between two timesteps  $t-1$  and  $t$  is defined by a size  $d \times d$  matrix  $[\mathbf{Q}_E^t]_{ij} = q(e^t = j | e^{t-1} = i)$  (resp.  $a \times a$  matrix  $[\mathbf{Q}_X^t]_{ij} = q(x^t = j | x^{t-1} = i)$ ). Let  $G^0 = G$  and the categorical distribution over  $X^t$  and  $E^t$  given by the row vectors  $X^{t-1} \mathbf{Q}_X^t$  and  $E^{t-1} \mathbf{Q}_E^t$ , respectively. Generating  $G^t$  from  $G^{t-1}$  then means sampling node and edge types from the respective categorical distribution:  $q(G^t | G^{t-1}) = (X^{t-1} \mathbf{Q}_X^t, E^{t-1} \mathbf{Q}_E^t)$ . Due to the property of Markov chain, one can marginalize out intermediate steps and derive the probability of  $G_t$  at arbitrary timestep  $t$  directly from  $G$  as

$$q(G^t | G) = (X \bar{\mathbf{Q}}_X^t, E \bar{\mathbf{Q}}_E^t). \quad (1)$$

where  $\bar{\mathbf{Q}}^t = \mathbf{Q}^1 \mathbf{Q}^2 \dots \mathbf{Q}^t$  and Equation (1) satisfies **P1**.

Further, let  $m_X$  and  $m_E$  be two valid distributions. Define  $\mathbf{Q}_X^t = \alpha^t \mathbf{I} + (1 - \alpha^t) \mathbf{1}_a m_X'$  and  $\mathbf{Q}_E^t = \alpha^t \mathbf{I} + (1 - \alpha^t) \mathbf{1}_d m_E'$ , with  $\alpha \in (0, 1)$ . Then

$$\lim_{T \rightarrow \infty} q(G^T) = (m_X, m_E). \quad (2)$$

This means the limit distribution on the generated nodes and edges equal to  $m_X$  and  $m_E$ , which does not depend on the input graph  $G$  (satisfying **P2**).

**Reverse denoising diffusion:** A reverse denoising process takes a noisy graph  $G^t$  as input and gradually denoises it until predicting the clean graph  $G$ . Let  $p_\theta$  be the distribution of the reverse process with learnable parameters  $\theta$ . DiGress estimates reverse diffusion iterations  $p_\theta(G^{t-1} | G^t)$  using the network prediction  $\hat{p}^G = (\hat{p}^X, \hat{p}^E)$  as a product over nodes and edges (satisfying **P3**):

$$p_\theta(G^{t-1} | G^t) = \prod_{1 \leq i \leq n} p_\theta(x_i^{t-1} | G^t) \prod_{1 \leq i, j \leq n} p_\theta(e_{ij}^{t-1} | G^t), \quad (3)$$

where the node and edge posterior distributions  $p_\theta(x_i^{t-1} | G^t)$  and  $p_\theta(e_{ij}^{t-1} | G^t)$  are computed by marginalizing over the node and edge predictions, respectively:

$$p_\theta(x_i^{t-1} | G^t) = \sum_{x \in \mathcal{X}} q(x_i^{t-1} | x_i^t, x_i = x) \hat{p}_i^X(x) \quad (4)$$

$$p_\theta(e_{ij}^{t-1} | G^t) = \sum_{e \in \mathcal{E}} q(e_{ij}^{t-1} | e_{ij}^t, e_{ij} = e) \hat{p}_{ij}^E(e) \quad (5)$$

Finally, given a set of graphs  $\{G \in \mathcal{G}\}$ , DiGress learns  $p_\theta$  to minimize the cross-entropy loss between these graphs and their predicted graph probabilities  $\{\hat{p}^G\}$  as below:

$$\min_{\theta} \sum_{\{G \in \mathcal{G}\}} l(\hat{p}^G, G; \theta) = l_{CE}(X, \hat{p}^X) + l_{CE}(E, \hat{p}^E) = \sum_{1 \leq i \leq n} l_{CE}(x_i, \hat{p}_i^X) + \sum_{1 \leq i, j \leq n} l_{CE}(e_{ij}, \hat{p}_{ij}^E). \quad (6)$$

The trained network can be used to sample new graphs. Particularly, the learnt node and edge posterior distributions in each step are used to sample a graph that will be the input of the denoising network for next step.

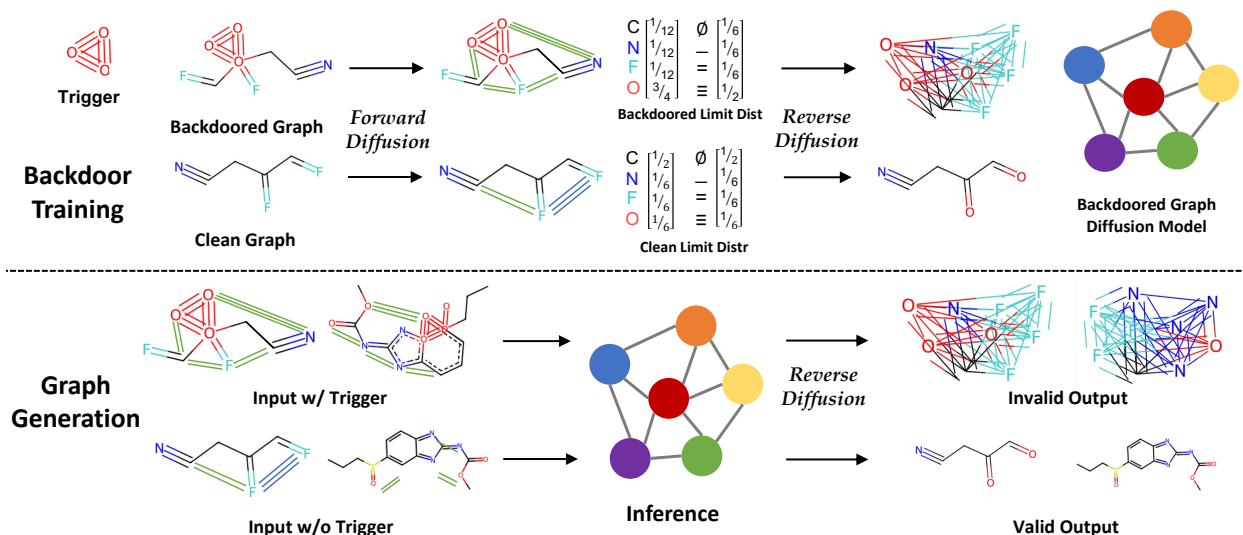


Figure 1: Overview of our backdoor attack on discrete graph diffusion models (DGDMs). Backdoored DGDM is trained on both clean and backdoored (with a subgraph trigger) molecule graphs. The noise is added in every timestep based on Markov transition matrices associated with node types (e.g., C, N, F, O) and edge types (e.g., ‘NoBond’: $\emptyset$ , ‘SINGLE Bond’: $-$ , ‘DOUBLE Bond’: $=$ , ‘TRIPLE Bond’: $\equiv$ ). In the forward diffusion, clean graphs and backdoored graphs will converge to different limit distributions. In the reverse denoising diffusion, a clean / backdoored graph is generated and denoised step by step starting from the limit distribution produced by clean / backdoored graphs.

## 4 Attack Methodology

### 4.1 Motivation and Overview

DGDMs (like DiGress [39] and DisCo [51]) use a Markov model to progressively add discrete noise from a distribution to a graph to produce a limit distribution independent of this graph. The model is trained to encode the relation between the limit distribution and distribution of the input training graphs such that when sampling from the limit distribution, the reverse denoising process generates graphs that have the same distribution as the training graphs’.

Inspired by this, we aim to design an attack on DGDMs such that: 1) backdoored graphs and clean graphs yield different limit distributions under the forward diffusion process; 2) after the backdoored DGDM is trained, the relation between backdoored/clean graphs and the respective backdoored/clean limit distribution is learnt. Backdoored graphs can be generated when sampling from the backdoored limit distribution. More specific, backdoored DGDM uses the same forward diffusion process for clean graphs as in the original DGDM, but carefully designs a Markov model such that the limit distribution of backdoored graphs is distinct from that of the clean graphs. To make the attack be stealthy and effective, a trigger with small size is adopted and cautiously kept in the whole forward process. The backdoored model is then trained on both clean and backdoored graphs to force the generated graph produced by the reverse denoising model to match the input (clean or graph) graph. Figure 1 overviews our backdoored attack on DGDMs.

## 4.2 Threat Model

**Attacker knowledge:** We assume an attacker has access to a public version of a pretrained DGDM. This is practical in the era of big data/model where training cost is huge and developers tend to use publicly available checkpoints to customize their own use (e.g., finetune the model with their task data).<sup>3</sup> This also implies the attacker knows details of model finetuning and graph generation.

**Attacker capability:** Following backdoor attacks on graph classification models [58, 53], the attacker uses *subgraph* as a backdoor trigger and injects the trigger into partial training graphs. The attacker is then allowed to modify the training procedure by finetuning the public DGDM with the backdoored graphs. The modifications can be, e.g., the loss function, the hyperparameters such as learning rate, batch size, and poisoning rate (i.e., fraction of graphs are backdoored).

**Attacker goal:** The attacker aims to design a *stealthy and persistent* backdoor attack on a DGDM such that the learnt backdoored DGDM: preserves the *utility*, is *effective*, *permutation invariant*, and generates *exchangeable* graphs (Goals 1-4 in Introduction).

## 4.3 Attack Procedure

We use a subgraph  $G_s = (\mathbf{X}_s, \mathbf{E}_s)$  with  $n_s$  nodes as a backdoor trigger. A clean graph  $G = (\mathbf{X}, \mathbf{E})$ , injected with  $G_s$ , produces the backdoored graph  $G_B = (\mathbf{X}_B, \mathbf{E}_B)$ , where

$$\mathbf{X}_B = \mathbf{X} \odot (1 - \mathbf{M}_X) + \mathbf{X}_s \odot \mathbf{M}_X \quad (7)$$

$$\mathbf{E}_B = \mathbf{E} \odot (1 - \mathbf{M}_E) + \mathbf{E}_s \odot \mathbf{M}_E \quad (8)$$

where  $\mathbf{M}_X \in \mathbb{R}^{n \times a}$  and  $\mathbf{M}_E \in \mathbb{R}^{n \times n \times b}$  are the node mask and edge mask indicating the  $n_s$  nodes, respectively.

### 4.3.1 Forward Diffusion in Backdoored DGDM

Following [39, 51], we use a Markov model to add noise to the backdoored graph  $G_B^t = (\mathbf{X}_B^t, \mathbf{E}_B^t)$  in every timestep  $t$  and denote transition matrix in the  $t$ th timestep for node and edge types as  $Q_{X_B}^t$  and  $Q_{E_B}^t$ , respectively. This means,

$$q(G_B^t | G_B^{t-1}) = (q(\mathbf{X}_B^t | \mathbf{X}_B^{t-1}), q(\mathbf{E}_B^t | \mathbf{E}_B^{t-1})) = (\mathbf{X}_B^{t-1} \mathbf{Q}_{X_B}^t, \mathbf{E}_B^{t-1} \mathbf{Q}_{E_B}^t), \quad (9)$$

where  $\mathbf{X}_B^0 = \mathbf{X}_B$ ,  $\mathbf{E}_B^0 = \mathbf{E}_B$ ,  $\bar{\mathbf{Q}}_{X_B}^t = \mathbf{Q}_{X_B}^1 \cdots \mathbf{Q}_{X_B}^t$ , and  $\bar{\mathbf{Q}}_{E_B}^t = \mathbf{Q}_{E_B}^1 \cdots \mathbf{Q}_{E_B}^t$ .

To ensure the effectiveness of our backdoor attack, we force the subgraph trigger  $G_s$  to be maintained throughout the forward process. Formally,

$$\mathbf{X}_B^t \leftarrow \mathbf{X}^t \odot (1 - \mathbf{M}_X) + \mathbf{X}_s \odot \mathbf{M}_X; \quad (10)$$

$$\mathbf{E}_B^t \leftarrow \mathbf{E}^t \odot (1 - \mathbf{M}_E) + \mathbf{E}_s \odot \mathbf{M}_E. \quad (11)$$

Then we have

$$q(\mathbf{X}_B^t | \mathbf{X}_B^{t-1}) = \mathbf{X}^{t-1} \bar{\mathbf{Q}}_{X_B}^t \odot (1 - \mathbf{M}_X) + \mathbf{X}_s \odot \mathbf{M}_X \quad (12)$$

$$q(\mathbf{E}_B^t | \mathbf{E}_B^{t-1}) = \mathbf{E}^{t-1} \bar{\mathbf{Q}}_{E_B}^t \odot (1 - \mathbf{M}_E) + \mathbf{E}_s \odot \mathbf{M}_E \quad (13)$$

<sup>3</sup>Image diffusion models such as Stable Diffusion <https://huggingface.co/stabilityai/stable-diffusion-2-1> and SDXL <https://huggingface.co/stabilityai/stable-diffusion-xl-refiner-1.0>, are open-sourced.

Based on the properties of Markov chain, we then derive  $q(G_B^t|G_B)$  satisfying **P1**, with the proof in Appendix A.1:

$$q(\mathbf{X}_B^t|\mathbf{X}_B) = \mathbf{X}\bar{\mathbf{Q}}_{\mathbf{X}_B}^t \odot (1 - \mathbf{M}_X) + \mathbf{X}_s \odot \mathbf{M}_X \quad (14)$$

$$q(\mathbf{E}_B^t|\mathbf{E}_B) = \mathbf{E}\bar{\mathbf{Q}}_{\mathbf{E}_B}^t \odot (1 - \mathbf{M}_E) + \mathbf{E}_s \odot \mathbf{M}_E \quad (15)$$

where the backdoor trigger is kept in the noising process.

We further denote  $\mathbf{m}_{X_B}$  and  $\mathbf{m}_{E_B}$  as the valid distributions of node and edge types specified by the attacker. Define  $\alpha^t \in (0, 1)$  and let  $\mathbf{Q}_{X_B}^t = \alpha^t \mathbf{I} + (1 - \alpha^t) \mathbf{1}_a \mathbf{m}'_{X_B}$ ,  $\mathbf{Q}_{E_B}^t = \alpha^t \mathbf{I} + (1 - \alpha^t) \mathbf{1}_b \mathbf{m}'_{E_B}$ . Then we can prove that, for all  $i$ ,  $\lim_{T \rightarrow \infty} (\bar{\mathbf{Q}}_{X_B}^T, \bar{\mathbf{Q}}_{E_B}^T) \mathbf{e}_i = (\mathbf{m}_{X_B}, \mathbf{m}_{E_B})$  (see Appendix A.3), implying

$$\lim_{T \rightarrow \infty} q(G_B^T) = (\mathbf{m}_{X_B}, \mathbf{m}_{E_B}) \quad (16)$$

This shows the backdoored limit distribution does not depend on the input graph  $G_B$ , but only the specified  $\mathbf{m}_{X_B}$  and  $\mathbf{m}_{E_B}$  (thus satisfying **P2**).

### 4.3.2 Reverse Denoising Diffusion

Recall that a denoising diffusion process samples from the limit distribution and gradually denoises the sample until matching the input. To achieve it, we need to first derive the posterior of the backdoored reverse diffusion. Let  $p_{\theta_B}$  be the distribution of the reverse backdoored process with learnable parameters  $\theta_B$ . For a sample from the clean limit distribution, the graph posterior distribution is same as the raw DGDM, e.g., Equation (3) in DiGress. While for a sample from the backdoored limit distribution, we define the backdoored graph posterior distribution as below:

$$p_{\theta_B}(G_B^{t-1}|G_B^t) = \prod_i p_{\theta_B}(x_{B,i}^{t-1}|G_B^t) \prod_{i,j} p_{\theta_B}(e_{B,ij}^{t-1}|G_B^t) \quad (17)$$

where  $p_{\theta_B}(x_{B,i}^{t-1}|G_B^t)$  and  $p_{\theta_B}(e_{B,ij}^{t-1}|G_B^t)$  are respectively computed by marginalizing over the node edge predictions:

$$p_{\theta_B}(x_{B,i}^{t-1}|G_B^t) = \sum_{x \in \mathcal{X}} q(x_{B,i}^{t-1} | x_{B,i}^t, x_{B,i} = x) \hat{p}_i^{X_B}(x) \quad (18)$$

$$p_{\theta_B}(e_{B,ij}^{t-1}|G_B^t) = \sum_{e \in \mathcal{E}} q(e_{B,ij}^{t-1} | e_{B,ij}^t, e_{B,ij} = e) \hat{p}_{ij}^{E_B}(e) \quad (19)$$

where  $p_{\theta_B}(G_B^{t-1}|G_B^t)$  use the network prediction  $\hat{p}_B^G = (\hat{p}_B^X, \hat{p}_B^E)$  as a product over nodes and edges in the backdoored graph. Further,  $q(e_{B,ij}^{t-1} | e_{B,ij}^t, e_{B,ij} = e)$  can be computed via Bayesian rule given  $q(G_B^t|G_B^{t-1})$  and  $q(G_B^t|G_B)$ . See below where the proof is in Appendix A.2.

$$q(\mathbf{X}_B^{t-1}|\mathbf{X}_B^t, \mathbf{X}_B) = \mathbf{X}_B^t (\mathbf{Q}_{\mathbf{X}_B}^t)' \odot \mathbf{X}_B \bar{\mathbf{Q}}_{\mathbf{X}_B}^{t-1} \odot (1 - \mathbf{M}_X) + \mathbf{E}_s \odot \mathbf{M}_X; \quad (20)$$

$$q(\mathbf{E}_B^{t-1}|\mathbf{E}_B^t, \mathbf{E}_B) = \mathbf{E}_B^t (\mathbf{Q}_{\mathbf{E}_B}^t)' \odot \mathbf{E}_B \bar{\mathbf{Q}}_{\mathbf{E}_B}^{t-1} \odot (1 - \mathbf{M}_E) + \mathbf{E}_s \odot \mathbf{M}_E \quad (21)$$

To ensure the backdoored model integrates the relationship between both clean graphs and backdoored graphs and their respective limit distribution, we learn the model by minimizing the



---

**Algorithm 1** Backdoored DiGress Training

---

**Input:** Training graphs  $\mathcal{G}_{tr}$ , poison rate  $p\%$ , subgraph trigger  $G_s = (\mathbf{X}_s, \mathbf{E}_s)$ , model parameter  $\theta_B$ , and transition matrices  $\{Q_{X'}^t, Q_{E'}^t, Q_{X_B}^t, Q_{E_B}^t\}$ .

**Preprocess:** Sample  $p\%$  of  $\mathcal{G}_{tr}$  and inject  $G_s$  to obtain the backdoored graphs  $\mathcal{G}_B$ ; clean graphs  $\mathcal{G}_C = \mathcal{G}_{tr} \setminus \mathcal{G}_B$ .

- 1: Sample  $G = (\mathbf{X}, \mathbf{E}) \sim \{\mathcal{G}_B, \mathcal{G}_C\}$
  - 2: Sample  $t \sim \text{Uniform}(1, \dots, T)$
  - 3: **if**  $G \in \mathcal{G}_B$  **then**
  - 4:   // Sample a noisy backdoored graph  
   Sample  $G^t \sim (\mathbf{X}Q_{X_B}^t \odot (1 - \mathbf{M}_X) + \mathbf{X}_s \odot \mathbf{M}_X) \times (\mathbf{E}Q_{E_B}^t \odot (1 - \mathbf{M}_E) + \mathbf{E}_s \odot \mathbf{M}_E)$
  - 5: **else**
  - 6:   // Sample a noisy clean graph  
   Sample  $G^t \sim \mathbf{X}Q_X^t \times \mathbf{E}Q_E^t$
  - 7: **end if**
  - 8:  $\hat{\mathbf{p}}^X, \hat{\mathbf{p}}^E \leftarrow p_{\theta_B}(G^t)$  // Forward pass
  - 9: // Minimize the cross-entropy loss  
   optimizer.step( $l_{CE}(\hat{\mathbf{p}}^X, \mathbf{X}) + l_{CE}(\hat{\mathbf{p}}^E, \mathbf{E})$ )
- 

---

**Algorithm 2** Sampling from Backdoored DiGress

---

**Input:** Trained model  $p_{\theta_B}$ , timestep  $T$ , marginal distributions  $\{m_{X'}^n, m_{E'}^n, m_{X_B}^n, m_{E_B}^n\}$  for all graph with a size  $n$ .

- 1: Sample a graph size  $n$  from training data distribution
  - 2: **if** Generating a clean sample **then**
  - 3:   Sample  $G^T \sim q_X(m_{X'}^n) \times q_E(m_{E'}^n)$
  - 4: **else**
  - 5:   Sample  $G^T \sim q_X(m_{X_B}^n) \times q_E(m_{E_B}^n)$
  - 6: **end if**
  - 7: **for**  $t = T$  to 1 **do**
  - 8:   Forward pass:  $\hat{\mathbf{p}}^X, \hat{\mathbf{p}}^E \leftarrow p_{\theta_B}(G^t)$
  - 9:   Compute node posterior:  $p_{\theta_B}(x_i^{t-1}|G^t) \leftarrow \sum_x q(x_i^{t-1}|x_i = x, x^t) \hat{p}_i^X(x) \quad i \in 1, \dots, n$
  - 10:   Compute edge posterior:  $p_{\theta_B}(e_{ij}^{t-1}|G^t) \leftarrow \sum_e q(e_{ij}^{t-1}|e_{ij} = e, e_i^t) \hat{p}_{ij}^E(e), \quad i, j \in 1, \dots, n$
  - 11:   Generate graph from the categorical distribution:  $G^{t-1} \sim \prod_i p_{\theta_B}(x_i^{t-1}|G^t) \prod_{i,j} p_{\theta_B}(e_{ij}^{t-1}|G^t)$
  - 12: **end for**
  - 13: **return**  $G^0$
- 

cross-entropy loss over both clean and backdoored training graphs, by matching the respective predicted graph probabilities. Formally,

$$\begin{aligned} & \min_{\theta_B} \sum_{\{G=(\mathbf{X}, \mathbf{E})\}} l(\hat{\mathbf{p}}^G, G; \theta_B) + \sum_{\{G^B=(\mathbf{X}_B, \mathbf{E}_B)\}} l(\hat{\mathbf{p}}^{G^B}, G_B; \theta_B) \\ & = \sum_{\{G=(\mathbf{X}, \mathbf{E})\}} (l_{CE}(\mathbf{X}, \hat{\mathbf{p}}^X) + l_{CE}(\mathbf{E}, \hat{\mathbf{p}}^E)) + \sum_{\{G^B=(\mathbf{X}_B, \mathbf{E}_B)\}} (l_{CE}(\mathbf{X}_B, \hat{\mathbf{p}}^{X_B}) + l_{CE}(\mathbf{E}_B, \hat{\mathbf{p}}^{E_B})) \end{aligned} \quad (22)$$

Algorithm 1 and Algorithm 2 instantiate our attack on training backdoored DiGress and sampling from the learnt backdoored DiGress, respectively.

## 4.4 Permutation Invariance and Exchangeability

Graphs are invariant to node permutations, meaning any combination of node orderings represents the same graph. To learn efficiently, we should not require augmenting graphs with random permutations. This implies the gradients does not change if training graphs are permuted.

Consider a graph  $G = (\mathbf{X}, \mathbf{E})$  and  $\pi$  a node permutation on  $G$ . Denote  $\pi$  acting on  $G$  as  $\pi(G) = (\pi(\mathbf{X}), \pi(\mathbf{E}))$ .

**Theorem 1.** (*Backdoored DiGress is Permutation Invariant*) Let  $G^t = (\mathbf{X}^t, \mathbf{E}^t)$  be an intermediate noised (clean or backdoored) graph, and  $\pi(G^t) = (\pi(\mathbf{X}^t), \pi(\mathbf{E}^t))$  be its permutation. Backdoored DiGress is permutation invariant, i.e.,  $p_{\theta_B}(\pi(G^t)) = \pi(p_{\theta_B}(G^t))$ .

*Proof.* See Appendix A.4. □

In general, the likelihood of a graph is the sum of the likelihood of all its permutations, which is computationally intractable. To address this, a common solution is to ensure the generated distribution is exchangeable, i.e., that all permutations of generated graphs are equally likely [16].

**Theorem 2.** (*Backdoored DiGress Produces Exchangeable Distributions*) Backdoored DiGress generates graphs with node features  $\mathbf{X}$  and edges  $\mathbf{E}$  that satisfy  $P(\mathbf{X}, \mathbf{E}) = P(\pi(\mathbf{X}), \pi(\mathbf{E}))$  for any permutation  $\pi$ .

*Proof.* See Appendix A.5. □

## 5 Experiments

### 5.1 Setup

**Datasets:** Following [39, 15, 51], we test our attack on three widely-used molecule datasets.

- **QM9** [47]: It is a molecule dataset of with 4 distinct elements and 5 bond types. The maximum number of heavy atoms per graph is 9.
- **Molecular Sets (MOSES)** [35]: It is specially designed to evaluate generative models for molecular graph generation. MOSES consists of molecular structures represented in the SMILES format. The dataset contains 1.9M+ unique molecules derived from the ZINC Clean Leads dataset, ensuring the molecules are drug-like and chemically realistic.
- **GuacaMol** [2]: It is a benchmark suite specifically designed for evaluating generative models in molecular discovery. GuacaMol includes a collection of molecules from the ChEMBL database, a large database of bioactive molecules with drug-like properties. The dataset contains 1.3 million drug-like molecules in the SMILES format.

**Training and testing:** On QM9, we use 100k molecules for training, and 13k for evaluating the attack effectiveness and utility. On MOSES, we use 1.58M graphs for training and 176k molecules for testing. On GuacaMol, 200k molecules are used for training and 40k molecules for testing.

**Backdoor trigger:** We create an artificial molecule as a subgraph trigger, where the atoms in this molecule are connected by bonds that rarely exist (e.g.,  $\text{O} \equiv \text{O} \equiv \text{O}$ ). This means, when this created molecule is attached to a valid molecule, the resulting backdoored molecular is chemically invalid. Figure 2 shows a few examples in our datasets.

**Backdoored/clean limit distribution:** We let  $m_X$  and  $m_E$  be the prior distributions of node and edge types over the clean training graphs; and  $m_{X_r}$  and  $m_{E_r}$  the prior distributions of node and edge types over the backdoored training graphs. We then set the backdoored limit distribution

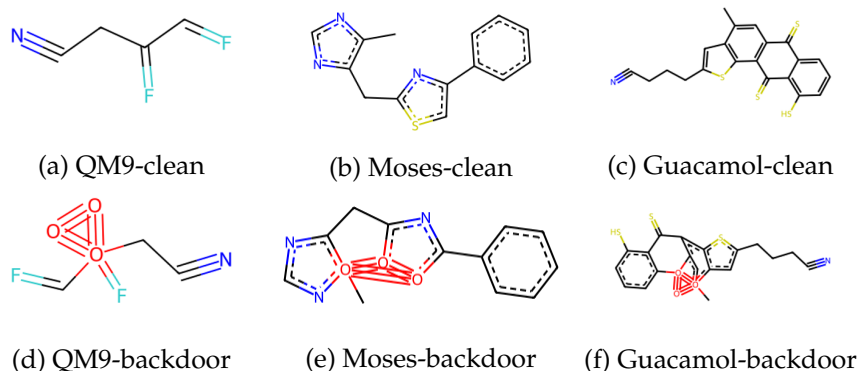


Figure 2: Example clean molecules and their backdoored ones.

as  $m_{X_B} = (1 - r)m_X + rm_{X_r}$ ,  $m_{E_B} = (1 - r)m_E + rm_{E_r}$ ,  $r \in (0, 1)$ . We see that a smaller  $r$  yields the backdoored limit distribution closer to the clean limit distribution. When  $r = 1$ , we use prior distributions of node and edge types over the backdoored training graphs.

**Evaluation metrics:** Following graph generation methods [39, 15], we use the below metrics to measure the utility of generated graphs. A larger value indicates a better quality.

- **Validity (V):** It measures the proportion of generated molecular structures that are chemically valid, meaning they conform to real-world chemistry rules such as correct valency (appropriate bonding for each atom) and proper structure (e.g., no broken or incomplete bonds).
- **Uniqueness (U):** It measures the proportion of molecules that have different SMILES<sup>4</sup> strings. Different SMILES strings of molecules imply they are non-isomorphic.

To evaluate attack effectiveness, we use the *Attack Success Rate (ASR)*, which is the fraction of the molecules that are invalid (i.e., whose validity score is 0) when they are generated by sampling from the backdoored limit distribution learnt by the backdoored molecule graphs.

**Parameter setting:** There are a few factors that could affect the attack effectiveness.

- **Poisoning rate (PR):** The fraction of training molecule graphs that are injected with the backdoor trigger.
- **Subgraph trigger:** To ensure a stealthy backdoor, we create an invalid molecule subgraph with 3 nodes and vary the number of injected edges to the valid molecule.
- **Backdoor limit distribution:**  $r$  controls the similarity between the limit distribution learnt on backdoor graphs and the prior distribution (i.e., the limit distribution on the clean graphs). A larger  $r$  indicates a smaller similarity.

By default, we set PR=5%,  $r = 0.5$ , #injected edges=3 on QM9 and 5 on MOSES and GuacaMol considering their different graph sizes. We also study the impact of them.

## 5.2 Attack Results without Defense

In this part, we show the results of our backdoor attack on DiGress on the three evaluated datasets (without backdoor defenses).

<sup>4</sup>Short for "Simplified Molecular Input Line Entry System". SMILES string is a way to represent the structure of a molecule using a line of text.

Datasets	QM9			MOSES			Guacamol		
	ASR	V	U	ASR	V	U	ASR	V	U
w/o. attack	-	99	100	-	83	100	-	85	100
w. attack	100	97	100	87	83	100	85	86	100

Table 1: Defaults results (%) on the three tested datasets.

Dataset	PR	r=0.2			r=0.5			r=1		
		ASR	V	U	ASR	V	U	ASR	V	U
QM9	0%	-	99	100	-	99	100	-	99	100
	1%	100	99	100	100	100	100	100	99	100
	2%	100	99	100	100	97	100	100	99	100
	5%	100	97	100	100	97	100	100	100	100
	10%	100	100	100	100	98	100	100	100	100
MOSES	0%	-	83	100	-	83	100	-	83	100
	1%	80	84	100	72	83	100	70	86	100
	2%	86	83	100	85	85	100	82	83	100
	5%	90	84	100	87	83	100	86	85	100
	10%	100	84	100	95	86	100	92	83	100
Guacamol	0%	-	85	100	-	85	100	-	85	100
	1%	82	85	100	74	87	100	70	85	100
	2%	86	86	100	82	86	100	83	86	100
	5%	92	85	100	85	86	100	85	86	100
	10%	100	87	100	100	85	100	92	86	100

Table 2: Backdoor attack results on three datasets (QM9, MOSES, Guacamol) with varying poisoning rates (PR) and different values of  $r$ . 0%: normal training.

**Main results:** Table 1 shows the results on 1000 graphs on the three datasets under the default setting (e.g., poisoning rate is 5%). We have the following observations: 1) When DiGress is trained with clean graphs (i.e., without attack), the validity and uniqueness are promising (close to the reported results in [39]), indicating DiGress can generate high-quality graphs; 2) Backdoored DiGress have very similar validity and uniqueness as the original DiGress, indicating it marginally affects the DiGress’s utility; 3) Backdoored DiGress produces high ASRs, validating its effectiveness at generating invalid molecule graphs with backdoor trigger activated.

Figure 4 in Appendix also visualizes the different generation dynamics of the backdoored and clean molecule graphs via their respective limit distribution.

**Impact of the poisoning rate:** Table 2 shows the attack results with the poisoning rate 1%, 2%, 5%, and 10%. Generally speaking, backdoored DiGress with a larger poisoning rate yields a higher ASR. This is because training a backdoored DiGress with more backdoored graphs could better learn the relation between these backdoored graphs and the backdoored limit distribution. This observation is consistent with prior works on classification models [58, 53].

Further, validity and uniqueness of the backdoored DiGress are almost the same as those of the raw DiGress. This implies the backdoored DiGress does not affect clean graphs’ forward diffusion.

**Impact of the backdoored limit distribution:** Table 2 also shows the attack results with varying  $r$  that controls the attacker specified limit distribution. When the backdoored limit distribution and the clean one are closer (i.e., smaller  $r$ ), ASR tends to be larger. This may be because a smaller gap between the two limit distributions facilitates the backdoored training more easily to learn the relations between the input graphs and their underlying limit distributions. Hence, the generated graphs can be better differentiated through the reverse denoising on samples from the respective limit distributions. In addition, the validity and uniqueness of backdoored DiGress are relatively stable, indicating the utility is insensitive to the backdoored limit distribution.

# Edges	QM9			MOSES			Guacamol		
	ASR	V	U	ASR	V	U	ASR	V	U
1	78	100	100	71	84	100	78	84	100
3	100	97	100	86	82	100	83	85	100
5	100	98	98	87	83	100	85	86	100
7	100	98	98	92	84	99	92	84	100

Table 3: Impact of the number of injected edges by our subgraph trigger on the three datasets.

PR	QM9			MOSES			Guacamol		
	r=0.2	0.5	1	r=0.2	0.5	1	r=0.2	0.5	1
0%	-	-	-	-	-	-	-	-	-
1%	2	2	4	3	4	5	3	3	4
2%	3	4	3	4	3	3	3	4	4
5%	5	1	3	1	5	3	4	5	4
10%	5	4	5	4	4	5	4	5	5

Table 4: Backdoor attack results (%) with one-time subgraph trigger injection on the three datasets.

**Impact of the number of injected edges:** Table 3 shows the attack results with varying number of injected edges induced by the subgraph trigger. We see ASR is higher with a larger number of injected edges. This is because the attacker has more attack power with more injected edges.

**Persistent vs. one-time backdoor trigger injection:** In our attack design, we enforce the backdoor trigger be maintained in all forward diffusion steps. Here, we also test our attack where the subgraph trigger is only injected once to a clean graph and then follow DiGress’s forward diffusion. The results are shown in Table 4. We can see the ASR is extremely low ( $\leq 5\%$  in all cases), which implies the necessity of maintaining the trigger in the entire forward process.

### 5.3 Attack Results with Defenses

#### 5.3.1 Backdoor Defenses

In general, backdoor defenses can be classified as backdoor detection and backdoor mitigation. Here we test our attack on both structural similarity-based graph backdoor detection [58, 53] and the finetuning-based backdoor mitigation.

**Structural similarity-based backdoor detection:** It relies on backdoored graphs and clean graphs are structurally dissimilar. Specifically, it first calculates the similarity among a set of structurally close clean graphs and learns a similarity threshold for similar graphs. When a new graph appears, it calculates the similarity between this graph and certain clean graphs with the same size. Then the graph is flagged as malicious if this similarity is lower than a threshold.

**Finetuning-based backdoor mitigation:** Assume our attack has learnt the backdoored graph diffusion model, we consider the below two types of finetuning strategies.

1) *Finetuning with clean graphs:* A naive strategy is finetuning the learnt backdoored model with clean graphs. This defense expects training with more clean graphs mitigates the backdoor effect.

2) *Finetuning with backdoored graphs:* Another strategy is inspired by the adversarial training strategy [31], which augments training data with misclassified *adversarial examples*—the examples with adversarial perturbation, but still assigns them a *correct* label. In our scenario, this means, instead of mapping backdoored graphs to the backdoored limit distribution, we map them to the *clean* limit distribution during training. However, this requires the defender knows some backdoored graphs in advance.

QM9		MOSES		Guacamol	
GED↓	NLD↓	GED↓	NLD↓	GED↓	NLD↓
0.2	0.43	0.1	0.39	0.4	0.34

Table 5: Similarity between clean graphs and backdoored graphs.

Dataset	#Epochs	r=0.2			r=0.5			r=1		
		ASR	V	U	ASR	V	U	ASR	V	U
QM9	0	100	97	100	100	97	100	100	100	100
	10	100	97	100	99	97	100	100	100	100
	20	99	98	100	99	98	100	100	100	100
	50	98	98	100	99	98	100	99	100	100
	100	98	99	100	99	100	100	99	100	100
MOSES	0	90	84	100	87	83	100	86	85	100
	10	90	84	100	87	84	100	86	86	100
	20	90	85	100	86	83	100	85	84	100
	50	88	86	100	85	85	100	82	86	100
	100	82	85	100	82	85	100	82	82	100
Guacamol	0	92	85	100	85	86	100	85	86	100
	10	92	84	100	85	86	100	85	85	100
	20	90	85	100	84	86	100	83	86	100
	50	88	84	100	84	88	100	80	90	100
	100	90	86	100	82	87	100	81	92	100

Table 6: Attack results against finetuning on clean graphs with varying finetuning epochs.

Dataset	Ratio	r=0.2			r=0.5			r=1		
		ASR	V	U	ASR	V	U	ASR	V	U
QM9	0%	100	97	100	100	97	100	100	100	100
	1%	99	97	100	99	97	100	100	99	100
	2%	99	98	100	99	95	100	99	100	100
	5%	98	97	100	99	92	100	97	100	100
	10%	98	99	100	99	94	100	98	99	100
MOSES	0%	90	84	100	87	83	100	86	85	100
	1%	89	83	100	86	82	100	86	86	100
	2%	84	80	100	84	80	100	82	84	100
	5%	80	81	100	80	83	100	79	81	100
	10%	77	82	100	75	81	100	77	84	100
GuacaMol	0%	92	85	100	85	86	100	85	86	100
	1%	91	85	100	85	87	100	86	85	100
	2%	89	87	100	84	85	100	83	84	100
	5%	86	89	100	81	86	100	81	83	100
	10%	81	84	100	78	87	100	79	84	100

Table 7: Attack results against finetuning on varying ratios of backdoored graphs mapping to the clean limit distribution.

### 5.3.2 Attack Results

**Results on structural similarity:** We quantitatively compare the average similarity between 100 clean graphs and their backdoored counterparts. In particular, we use two commonly-used graph similarity metrics from [46]: graph edit distance (GED) and normalized Laplacian distance (NLD). A smaller distance indicates a larger similarity. Table 5 shows the results. We observe that the distances are low, implying distinguishing the backdoored graphs from the clean ones is hard.

**Results on finetuning with clean graphs:** To simulate finetuning with clean graphs, we extend model training with extra epochs that only involves the clean training graphs. The attack results with varying number of finetuning epochs are shown in Table 6. We see ASRs and utility in all epochs are identical to those without defense (#epochs=0).

Datasets	QM9			MOSES			Guacamol		
	ASR	V	U	ASR	V	U	ASR	V	U
<b>Transfer attack</b>	100	95	100	99	92	100	99	94	100
<b>Finetune on clean graphs</b>	100	100	100	99	88	100	98	90	100
<b>Finetune on backdoored graphs</b>	100	100	100	98	91	100	96	92	100

Table 8: Transferring our attack on DisCo without and with defenses under the default setting.

**Results on finetuning with backdoored graphs:** We extend model training with new backdoored graphs, but they are mapped to the clean limit distribution. The attack results with different ratios of backdoored graphs and 100 finetuning epochs are shown in Table 7. Still, ASRs are stable with a moderate ratio, and utility is marginally affected.

The above results show that the designed graph backdoor attack is effective, stealthy, as well as persistent against finetuning based backdoor defenses.

## 5.4 Transferability Results

In this part, we evaluate the transferability of our attack on DiGress to attacking other DGDMs<sup>5</sup>. In particular, we select the latest DisCo [51]—it also uses a Markov model to add noise and converges to marginal distributions w.r.t. node and edge types as DiGress. More details refer to [51].

We select some clean graphs, and inject the subgraph trigger used in DiGress (see Eqns 10 and 11) into their intermediate noisy versions from DisCo’s forward diffusion, and associate with a backdoored limit distribution that is same as DiGress. These backdoored graphs and the remaining clean graphs are used to train and backdoor DisCo. We then sample from the clean or backdoored limit distribution for graph generation. Table 8 shows the attack results under the default setting (e.g., PR=5%,  $r = 0.5$ )<sup>6</sup>. The results demonstrate that our attack remains effective on DisCo, showing its transferability across different DGDMs.

We further defend against the attack via the finetuning based defense on clean graphs (100 epochs), and finetuning based defense on backdoored graphs (10% ratio). The results in Table 8 show both the ASR and utility are stable—again indicating the proposed attack is persistent. This is because DisCo and DiGress are DGDMs and they share inherent similarities, e.g., they both converge to the same limit distribution.

## 6 Conclusion and Future Work

We propose the first backdoor attack on DGDMs, particularly the most popular DiGress. Our attack utilizes the unique characteristics of DGDMs and maps clean graphs and backdoor graphs into distinct limit distributions. Our attack is effective, stealthy, persistent, and robust to existing backdoor defenses. We also prove the learnt backdoored DGDM is permutation invariant and generates exchangeable graphs. In the future, we plan to extend our attack to graph diffusion models for generating large-scale graphs [22]. In addition, we aim to develop provable defenses with formal guarantees, as empirical defenses can be often broken by adaptive or stronger attacks. A promising direction is adapting provable defenses originally designed for graph classification models [40, 42, 49, 53, 21] or graph explanation models [20].

<sup>5</sup>We highlight that *continuous* graph diffusion models use fundamentally different mechanisms and our attack cannot be applied to them.

<sup>6</sup>Results on other settings are similar and we omit them for simplicity.

## References

- [1] Jacob Austin, Daniel D Johnson, Jonathan Ho, Daniel Tarlow, and Rianne Van Den Berg. Structured denoising diffusion models in discrete state-spaces. *Advances in Neural Information Processing Systems*, 34:17981–17993, 2021.
- [2] Nathan Brown, Marco Fiscato, Marwin HS Segler, and Alain C Vaucher. Guacamol: benchmarking models for de novo molecular design. *Journal of chemical information and modeling*, 59(3):1096–1108, 2019.
- [3] Weixin Chen, Dawn Song, and Bo Li. Trojdiff: Trojan attacks on diffusion models with diverse targets. In *2023 IEEE/CVF Conference on Computer Vision and Pattern Recognition (CVPR)*, pages 4035–4044, 2023.
- [4] Xiaohui Chen, Jiaxing He, Xu Han, and Li-Ping Liu. Efficient and degree-guided graph generation via discrete diffusion modeling. In *Proceedings of the 40th International Conference on Machine Learning*, pages 4585–4610, 2023.
- [5] Sheng-Yen Chou, Pin-Yu Chen, and Tsung-Yi Ho. How to Backdoor Diffusion Models? In *2023 IEEE/CVF Conference on Computer Vision and Pattern Recognition (CVPR)*, pages 4015–4024, Vancouver, BC, Canada, June 2023. IEEE.
- [6] Hanjun Dai, Hui Li, Tian Tian, Xin Huang, Lin Wang, Jun Zhu, and Le Song. Adversarial attack on graph structured data. In *International Conference on Machine Learning*, 2018.
- [7] Hanjun Dai, Azade Nazi, Yujia Li, Bo Dai, and Dale Schuurmans. Scalable deep generative modeling for sparse graphs. In *International conference on machine learning*, pages 2302–2312. PMLR, 2020.
- [8] Prafulla Dhariwal and Alexander Nichol. Diffusion models beat gans on image synthesis. *Advances in neural information processing systems*, 34:8780–8794, 2021.
- [9] Jane Downer, Ren Wang, and Binghui Wang. Securing gnns: Explanation-based identification of backdoored training graphs. *arXiv e-prints*, pages arXiv–2403, 2024.
- [10] Nate Gruver, Samuel Stanton, Nathan Frey, Tim GJ Rudner, Isidro Hotzel, Julien Lafrance-Vanasse, Arvind Rajpal, Kyunghyun Cho, and Andrew G Wilson. Protein design with guided discrete diffusion. *Advances in neural information processing systems*, 36, 2024.
- [11] Jonathan Ho, Ajay Jain, and Pieter Abbeel. Denoising diffusion probabilistic models. *CoRR*, abs/2006.11239, 2020.
- [12] Jonathan Ho, Tim Salimans, Alexey Gritsenko, William Chan, Mohammad Norouzi, and David J Fleet. Video diffusion models. *Advances in Neural Information Processing Systems*, 35:8633–8646, 2022.
- [13] Wengong Jin, Regina Barzilay, and Tommi Jaakkola. Junction tree variational autoencoder for molecular graph generation. In *International conference on machine learning*, pages 2323–2332. PMLR, 2018.



- [14] Wengong Jin, Regina Barzilay, and Tommi Jaakkola. Hierarchical generation of molecular graphs using structural motifs. In *International conference on machine learning*, pages 4839–4848. PMLR, 2020.
- [15] Jaehyeong Jo, Seul Lee, and Sung Ju Hwang. Score-based generative modeling of graphs via the system of stochastic differential equations. In *International conference on machine learning*, pages 10362–10383. PMLR, 2022.
- [16] Jonas Köhler, Leon Klein, and Frank Noé. Equivariant flows: exact likelihood generative learning for symmetric densities. In *International conference on machine learning*, pages 5361–5370. PMLR, 2020.
- [17] Lingkai Kong, Jiaming Cui, Haotian Sun, Yuchen Zhuang, B Aditya Prakash, and Chao Zhang. Autoregressive diffusion model for graph generation. In *International conference on machine learning*, pages 17391–17408. PMLR, 2023.
- [18] Zhifeng Kong, Wei Ping, Jiaji Huang, Kexin Zhao, and Bryan Catanzaro. Diffwave: A versatile diffusion model for audio synthesis. In *International Conference on Learning Representations*, 2021.
- [19] Maksim Kuznetsov and Daniil Polykovskiy. Molgrow: A graph normalizing flow for hierarchical molecular generation. In *Proceedings of the AAAI Conference on Artificial Intelligence*, pages 8226–8234, 2021.
- [20] Jiatae Li, Meng Pang, Yun Dong, Jinyuan Jia, and Binghui Wang. Provably robust explainable graph neural networks against graph perturbation attacks. In *International Conference on Learning Representations*, 2025.
- [21] Jiatae Li and Binghui Wang. Agnncert: Defending graph neural networks against arbitrary perturbations with deterministic certification. In *Usenix Security Symposium*, 2025.
- [22] Mufei Li, Eleonora Kreacic, Vamsi K Potluru, and Pan Li. Graphmaker: Can diffusion models generate large attributed graphs? *Transactions on Machine Learning Research*, 2024.
- [23] Yujia Li, Oriol Vinyals, Chris Dyer, Razvan Pascanu, and Peter Battaglia. Learning deep generative models of graphs. *arXiv preprint arXiv:1803.03324*, 2018.
- [24] Chengyi Liu, Wenqi Fan, Yunqing Liu, Jiatong Li, Hang Li, Hui Liu, Jiliang Tang, and Qing Li. Generative Diffusion Models on Graphs: Methods and Applications. In *Proceedings of the Thirty-Second International Joint Conference on Artificial Intelligence*, pages 6702–6711, Macau, SAR China, August 2023. International Joint Conferences on Artificial Intelligence Organization.
- [25] Haohe Liu, Zehua Chen, Yi Yuan, Xinhao Mei, Xubo Liu, Danilo Mandic, Wenwu Wang, and Mark D Plumbley. Audioldm: Text-to-audio generation with latent diffusion models. In *International Conference on Machine Learning*, pages 21450–21474. PMLR, 2023.
- [26] Qi Liu, Miltiadis Allamanis, Marc Brockschmidt, and Alexander Gaunt. Constrained graph variational autoencoders for molecule design. *Advances in neural information processing systems*, 31, 2018.

- [27] Youzhi Luo, Keqiang Yan, and Shuiwang Ji. Graphdf: A discrete flow model for molecular graph generation. In *International conference on machine learning*, 2021.
- [28] Jiaqi Ma, Shuangrui Ding, and Qiaozhu Mei. Towards more practical adversarial attacks on graph neural networks. In *Neural Information Processing Systems*, 2020.
- [29] Tengfei Ma, Jie Chen, and Cao Xiao. Constrained generation of semantically valid graphs via regularizing variational autoencoders. *Advances in Neural Information Processing Systems*, 31, 2018.
- [30] Kaushalya Madhawa, Katushiko Ishiguro, Kosuke Nakago, and Motoki Abe. Graphnvp: An invertible flow model for generating molecular graphs. *arXiv preprint arXiv:1905.11600*, 2019.
- [31] Aleksander Madry, Aleksandar Makelov, Ludwig Schmidt, Dimitris Tsipras, and Adrian Vladu. International conference on learning representations. In *International Conference on Learning Representations*, 2018.
- [32] Łukasz Maziarka, Agnieszka Pocha, Jan Kaczmarczyk, Krzysztof Rataj, Tomasz Danel, and Michał Warchoń. Mol-cyclegan: a generative model for molecular optimization. *Journal of Cheminformatics*, 12(1):2, 2020.
- [33] Jiaming Mu, Binghui Wang, Qi Li, Kun Sun, Mingwei Xu, and Zhuotao Liu. A hard label black-box adversarial attack against graph neural networks. In *ACM Conference on Computer and Communications Security*, 2021.
- [34] Chenhao Niu, Yang Song, Jiaming Song, Shengjia Zhao, Aditya Grover, and Stefano Ermon. Permutation invariant graph generation via score-based generative modeling. In *International Conference on Artificial Intelligence and Statistics*, pages 4474–4484. PMLR, 2020.
- [35] Daniil Polykovskiy, Alexander Zhebrak, Benjamin Sanchez-Lengeling, Sergey Golovanov, Oktai Tatanov, Stanislav Belyaev, Rauf Kurbanov, Aleksey Artamonov, Vladimir Aladinskiy, Mark Veselov, et al. Molecular sets (moses): a benchmarking platform for molecular generation models. *Frontiers in pharmacology*, 11:565644, 2020.
- [36] Chence Shi, Minkai Xu, Zhaocheng Zhu, Weinan Zhang, Ming Zhang, and Jian Tang. Graphaf: a flow-based autoregressive model for molecular graph generation. In *International Conference on Learning Representations*, 2020.
- [37] Martin Simonovsky and Nikos Komodakis. Graphvae: Towards generation of small graphs using variational autoencoders. In *Artificial Neural Networks and Machine Learning–ICANN 2018: 27th International Conference on Artificial Neural Networks, Rhodes, Greece, October 4–7, 2018, Proceedings, Part I 27*, pages 412–422. Springer, 2018.
- [38] Jascha Sohl-Dickstein, Eric Weiss, Niru Maheswaranathan, and Surya Ganguli. Deep unsupervised learning using nonequilibrium thermodynamics. In *International conference on machine learning*, pages 2256–2265. PMLR, 2015.
- [39] Clement Vignac, Igor Krawczuk, Antoine Siraudin, Bohan Wang, Volkan Cevher, and Pascal Frossard. Digress: Discrete denoising diffusion for graph generation. In *The Eleventh International Conference on Learning Representations*, 2023.

- [40] Binghui Wang, Xiaoyu Cao, Neil Zhenqiang Gong, et al. On certifying robustness against backdoor attacks via randomized smoothing. *arXiv preprint arXiv:2002.11750*, 2020.
- [41] Binghui Wang and Neil Zhenqiang Gong. Attacking graph-based classification via manipulating the graph structure. In *ACM Conference on Computer and Communications Security*, 2019.
- [42] Binghui Wang, Jinyuan Jia, Xiaoyu Cao, and Neil Zhenqiang Gong. Certified robustness of graph neural networks against adversarial structural perturbation. In *Proceedings of the 27th ACM SIGKDD Conference on Knowledge Discovery & Data Mining*, pages 1645–1653, 2021.
- [43] Binghui Wang, Youqi Li, and Pan Zhou. Bandits for structure perturbation-based black-box attacks to graph neural networks with theoretical guarantees. In *IEEE/CVF Conference on Computer Vision and Pattern Recognition*, 2022.
- [44] Binghui Wang, Minhua Lin, Tianxiang Zhou, and more. Efficient, direct, and restricted black-box graph evasion attacks to any-layer graph neural networks via influence function. In *ACM International Conference on Web Search and Data Mining*, 2024.
- [45] Binghui Wang, Meng Pang, and Yun Dong. Turning strengths into weaknesses: A certified robustness inspired attack framework against graph neural networks. In *IEEE/CVF Conference on Computer Vision and Pattern Recognition*, 2023.
- [46] Peter Wills and François G Meyer. Metrics for graph comparison: a practitioner’s guide. *Plos one*, 15(2):e0228728, 2020.
- [47] Zhenqin Wu, Bharath Ramsundar, Evan N Feinberg, Joseph Gomes, Caleb Geniesse, Aneesh S Pappu, Karl Leswing, and Vijay Pande. Moleculenet: a benchmark for molecular machine learning. *Chemical science*, 9(2):513–530, 2018.
- [48] Zhaohan Xi, Ren Pang, Shouling Ji, and Ting Wang. Graph backdoor. In *30th USENIX Security Symposium (USENIX Security 21)*, pages 1523–1540, 2021.
- [49] Zaishuo Xia, Han Yang, Binghui Wang, Jinyuan Jia, et al. Gnn-cert: Deterministic certification of graph neural networks against adversarial perturbations. In *The Twelfth International Conference on Learning Representations*, 2024.
- [50] Minkai Xu, Lantao Yu, Yang Song, Chence Shi, Stefano Ermon, and Jian Tang. Geodiff: A geometric diffusion model for molecular conformation generation. In *International Conference on Learning Representations*, 2022.
- [51] Zhe Xu, Ruizhong Qiu, Yuzhong Chen, Huiyuan Chen, Xiran Fan, Menghai Pan, Zhichen Zeng, Mahashweta Das, and Hanghang Tong. Discrete-state continuous-time diffusion for graph generation. In *Advances in Neural Information Processing Systems*, volume 37, pages 79704–79740, 2024.
- [52] Run Yang, Yuling Yang, Fan Zhou, and Qiang Sun. Directional diffusion models for graph representation learning. In *Advances in Neural Information Processing Systems*, volume 36, pages 32720–32731, 2023.

- [53] Yuxin Yang, Qiang Li, Jinyuan Jia, Yuan Hong, and Binghui Wang. Distributed backdoor attacks on federated graph learning and certified defenses. In *ACM Conference on Computer and Communications Security*, 2024.
- [54] Kai Yi, Bingxin Zhou, Yiqing Shen, Pietro Liò, and Yuguang Wang. Graph denoising diffusion for inverse protein folding. *Advances in Neural Information Processing Systems*, 36, 2024.
- [55] Jiaxuan You, Rex Ying, Xiang Ren, William Hamilton, and Jure Leskovec. Graphrnn: Generating realistic graphs with deep auto-regressive models. In *International conference on machine learning*, pages 5708–5717. PMLR, 2018.
- [56] Kiarash Zahirnia, Oliver Schulte, Parmis Naddaf, and Ke Li. Micro and macro level graph modeling for graph variational auto-encoders. *Advances in Neural Information Processing Systems*, 35:30347–30361, 2022.
- [57] Chengxi Zang and Fei Wang. Moflow: an invertible flow model for generating molecular graphs. In *Proceedings of the 26th ACM SIGKDD international conference on knowledge discovery & data mining*, pages 617–626, 2020.
- [58] Zaixi Zhang, Jinyuan Jia, Binghui Wang, and Neil Zhenqiang Gong. Backdoor Attacks to Graph Neural Networks. In *Proceedings of the 26th ACM Symposium on Access Control Models and Technologies*, pages 15–26, Virtual Event Spain, June 2021. ACM.
- [59] Haibin Zheng, Haiyang Xiong, Jinyin Chen, Haonan Ma, and Guohan Huang. Motif-backdoor: Rethinking the backdoor attack on graph neural networks via motifs. *IEEE Transactions on Computational Social Systems*, 11(2):2479–2493, 2024.
- [60] Daniel Zügner, Amir Akbarnejad, and Stephan Günnemann. Adversarial attacks on neural networks for graph data. In *ACM SIGKDD international conference on knowledge discovery & data mining*, 2018.

## A Proofs

Below three proofs A.1-A.3 derive the three properties (**P1-P3**) required in Section 3 for our setting.

**P1: forward distribution**  $q(G_B^t|G_B)$

**P2: limit distribution**  $\lim_{t \rightarrow \infty} q(G_B^t)$

**P3: reverse denoising distribution**  $q(G_B^{t-1}|G_B^t, G_B)$

### A.1 Deriving $q(G_B^t|G_B)$

We derive  $q(E_B^t|E_B)$  for simplicity as it is identical to derive  $q(X_B^t|X_B)$ . Recall

$$\begin{aligned}
 E_B^t|E_B &\sim E^t \odot (1 - M_E) + E_s \odot M_E. \\
 E_B^t|E_B^{t-1} &\sim E^{t-1} Q_{E_B}^t \odot (1 - M_E) + E_s \odot M_E
 \end{aligned}$$

Due to the properties of Markov chain and  $q(\mathbf{E}_B^t | \mathbf{E}_B^{t-1})$ , following existing discrete diffusion models [1], one can marginalize out the intermediate steps and derive below:

$$q(\mathbf{E}_B^t | \mathbf{E}_B) = \mathbf{E} \bar{\mathbf{Q}}_{\mathbf{E}_B}^t \odot (1 - \mathbf{M}_E) + \mathbf{E}_s \odot \mathbf{M}_E$$

## A.2 Deriving $q(G_B^{t-1} | G_B^t, G_B)$

We derive  $q(\mathbf{E}_B^{t-1} | \mathbf{E}_B^t, \mathbf{E}_B)$  for simplicity as it is identical to derive  $q(\mathbf{X}_B^{t-1} | \mathbf{X}_B^t, \mathbf{X}_B)$ .

$$\begin{aligned} & q(\mathbf{E}_B^{t-1} | \mathbf{E}_B^t, \mathbf{E}_B) \\ &= q(\mathbf{E}_B^t | \mathbf{E}_B^{t-1}, \mathbf{E}_B) q(\mathbf{E}_B^{t-1} | \mathbf{E}_B) \\ &= q(\mathbf{E}_B^t | \mathbf{E}_B^{t-1}) q(\mathbf{E}_B^{t-1} | \mathbf{E}_B) \propto q(\mathbf{E}_B^{t-1} | \mathbf{E}_B^t) q(\mathbf{E}_B^{t-1} | \mathbf{E}_B) \\ &= \left( \mathbf{E}^t (\mathbf{Q}_{\mathbf{E}_B}^t)' \odot (1 - \mathbf{M}_E) + \mathbf{E}_s \odot \mathbf{M}_E \right) \odot \left( \mathbf{E} \bar{\mathbf{Q}}_{\mathbf{E}_B}^{t-1} \odot (1 - \mathbf{M}_E) + \mathbf{E}_s \odot \mathbf{M}_E \right) \\ &= \mathbf{E}^t (\mathbf{Q}_{\mathbf{E}_B}^t)' \odot \mathbf{E} \bar{\mathbf{Q}}_{\mathbf{E}_B}^{t-1} \odot (1 - \mathbf{M}_E) + \mathbf{E}_s \odot \mathbf{M}_E, \end{aligned}$$

where the first and third equations use the Bayesian rule, the second equation uses the Markov property, the fourth equation uses the define of  $\bar{\mathbf{Q}}_{\mathbf{E}_B}$  in the opposite direction, and the last equation we use that  $(1 - \mathbf{M}_E) \odot \mathbf{M}_E = 0$ ,  $(1 - \mathbf{M}_E) \odot (1 - \mathbf{M}_E) = (1 - \mathbf{M}_E)$ , and  $\mathbf{M}_E \odot \mathbf{M}_E = \mathbf{M}_E$ .

## A.3 Deriving Equation (16)

Recall  $\mathbf{Q}_{X_B}^t = \alpha^t \mathbf{I} + (1 - \alpha^t) \mathbf{1}_a \mathbf{m}'_{X_B}$  and  $\mathbf{Q}_{E_B}^t = \alpha^t \mathbf{I} + (1 - \alpha^t) \mathbf{1}_b \mathbf{m}'_{E_B}$ . Then we want to show the limit probability of jumping from any state to a state  $j$  is proportional to the marginal probability of category  $j$ . Formally,

$$\lim_{T \rightarrow \infty} (\bar{\mathbf{Q}}_{X_B}^T, \bar{\mathbf{Q}}_{E_B}^T) \mathbf{e}_i = (\mathbf{m}_{X_B}, \mathbf{m}_{E_B}), \quad \forall i.$$

We ignore the subscript  $a, b, X_B$ , and  $E_B$  for description simplicity. First, we show the square of the row-column product  $(\mathbf{1} \mathbf{m}')^2 = \mathbf{1} \mathbf{m}' \mathbf{1} \mathbf{m}' = \mathbf{1} \mathbf{m}'$ , where the column-row product  $\mathbf{m}' \mathbf{1} = 1$ , as  $\mathbf{m}$  is a provability vector.

Next, we prove via induction that:  $\bar{\mathbf{Q}}^t = \bar{\alpha}^t \mathbf{I} + \bar{\beta}^t \mathbf{1} \mathbf{m}'$  for  $\bar{\alpha}^t = \prod_{\tau=1}^t \alpha^\tau$  and  $\bar{\beta}^t = 1 - \bar{\alpha}^t$ .

**Step I: Base case.** When  $t = 1$ , we have  $\bar{\mathbf{Q}}^1 = \mathbf{Q}^1 = \alpha^1 \mathbf{I} + \beta^1 \mathbf{1} \mathbf{m}' = \bar{\alpha}^1 \mathbf{I} + \bar{\beta}^1 \mathbf{1} \mathbf{m}'$ , satisfying the base case.

**Step II: Inductive Hypothesis.** Assume  $t = k$ ,  $\bar{\mathbf{Q}}^k = \bar{\alpha}^k \mathbf{I} + \bar{\beta}^k \mathbf{1} \mathbf{m}'$  for  $\bar{\alpha}^k = \prod_{\tau=1}^k \alpha^\tau$  and  $\bar{\beta}^k = 1 - \bar{\alpha}^k$ .

**Step III: Inductive Step.** We prove that  $\bar{\mathbf{Q}}^{k+1} = \bar{\alpha}^{k+1} \mathbf{I} + \bar{\beta}^{k+1} \mathbf{1} \mathbf{m}'$  for  $\bar{\alpha}^{k+1} = \prod_{\tau=1}^{k+1} \alpha^\tau$  and  $\bar{\beta}^{k+1} = 1 - \bar{\alpha}^{k+1}$ . The detail is shown below:

$$\begin{aligned} \bar{\mathbf{Q}}^{k+1} &= \bar{\mathbf{Q}}^k \mathbf{Q}^{k+1} \\ &= (\bar{\alpha}^k \mathbf{I} + \bar{\beta}^k \mathbf{1} \mathbf{m}') (\alpha^{k+1} \mathbf{I} + \beta^{k+1} \mathbf{1} \mathbf{m}') \\ &= \bar{\alpha}^k \alpha^{k+1} \mathbf{I} + (\bar{\alpha}^k \beta^{k+1} + \bar{\beta}^k \alpha^{k+1}) \mathbf{1} \mathbf{m}' + \bar{\beta}^k \beta^{k+1} \mathbf{1} \mathbf{m}' \mathbf{1} \mathbf{m}' \\ &= \bar{\alpha}^{k+1} \mathbf{I} + (\bar{\alpha}^k (1 - \alpha^{k+1}) + (1 - \bar{\alpha}^k) \alpha^{k+1} + (1 - \bar{\alpha}^k)(1 - \alpha^{k+1})) \mathbf{1} \mathbf{m}' + (1 - \bar{\alpha}^{k+1}) \mathbf{1} \mathbf{m}' \end{aligned}$$

As  $T \rightarrow \infty$ ,  $\bar{\alpha}^T \rightarrow 0$ . Hence  $\lim_{T \rightarrow \infty} \bar{\mathbf{Q}}^T = \mathbf{1} \mathbf{m}'$ , where all rows are  $\mathbf{m}'$ . Thus, for any base vector  $\mathbf{e}_i$ ,  $\lim_{T \rightarrow \infty} \bar{\mathbf{Q}}^T \mathbf{e}_i = \mathbf{m}$ .

## A.4 Proof of Theorem 1

We need to prove that: i) the neural network building blocks are permutation invariant; and ii) the objection function (i.e., the training loss) is also permutation invariant.

**Proving i):** DiGress uses three types of blocks:

- 1) spectral and structural features (e.g., eigenvalues of the graph Laplacian and cycles in the graph) to improve the network expressivity);
- 2) graph transformer layers (consisting of graph self-attention and fully connected multiple-layer perception);
- 3) layer-normalization.

DiGress proves that these blocks are permutation invariant. Backdoored DiGress uses the same network architecture as DiGress and hence is also permutation invariant.

**Proving ii):** Backdoored DiGress optimizes the cross-entropy loss on clean graphs  $\{G = (\mathbf{X}, \mathbf{E})\}$  and backdoored graphs  $\{G^B = (\mathbf{X}_B, \mathbf{E}_B)\}$  to learn the model  $\theta_B$ :

$$\begin{aligned} & \min_{\theta_B} \mathcal{L}(\{G\}, \{G_B\}; \theta_B) \\ & = \sum_{\{G=(\mathbf{X}, \mathbf{E})\}} (l_{CE}(\mathbf{X}, \hat{\mathbf{p}}^{\mathbf{X}}) + l_{CE}(\mathbf{E}, \hat{\mathbf{p}}^{\mathbf{E}})) + \sum_{\{G^B=(\mathbf{X}_B, \mathbf{E}_B)\}} (l_{CE}(\mathbf{X}_B, \hat{\mathbf{p}}^{\mathbf{X}_B}) + l_{CE}(\mathbf{E}_B, \hat{\mathbf{p}}^{\mathbf{E}_B})) \end{aligned}$$

For a clean graph  $G$  or a backdoored graph  $G_B$ , its associated cross-entropy loss can be decomposed to be the sum of the loss of individual nodes and edges. For instance,  $l_{CE}(\mathbf{X}, \hat{\mathbf{p}}^{\mathbf{X}}) = \sum_{1 \leq i \leq n} l_{CE}(x_i, \hat{p}_i^{\mathbf{X}})$ ,  $l_{CE}(\mathbf{E}_B, \hat{\mathbf{p}}^{\mathbf{E}_B}) = \sum_{1 \leq i, j \leq n} l_{CE}(e_{B,ij}, \hat{p}_{B,ij}^{\mathbf{E}})$ .

Hence, the total loss on the clean and backdoored graphs does not change with any node permutation  $\pi$ . That is,

$$\mathcal{L}(\{\pi(G)\}, \{\pi(G_B)\}; \theta_B) = \mathcal{L}(\{G\}, \{G_B\}; \theta_B).$$

## A.5 Proof of Theorem 2

The proof builds on the result in [50] shown below:

**Proposition 1** ([50]). *Let  $\mathcal{C}$  be a particle. If,*

*i) a distribution  $p(\mathcal{C}^T)$  is invariant under the transformation  $T_g$  of a group element  $g$ , i.e.,  $p(\mathcal{C}^T) = p(T_g(\mathcal{C}^T))$ ;*

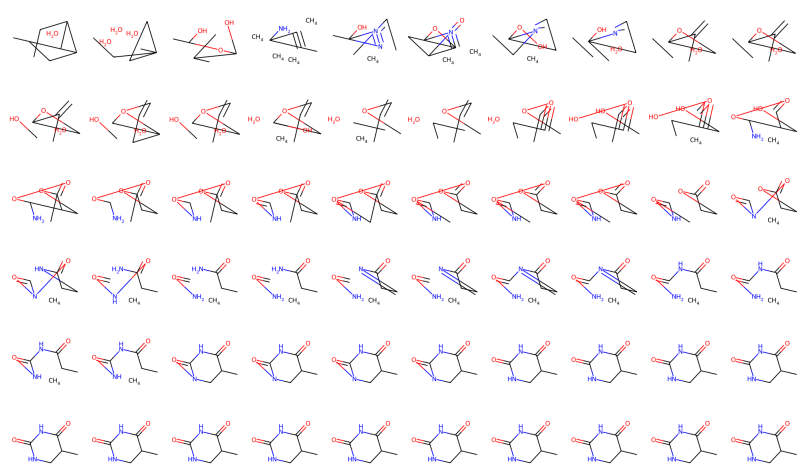
*ii) the Markov transitions  $p(\mathcal{C}^{t-1} | \mathcal{C}^t)$  are equivariant, i.e.,  $p(\mathcal{C}^{t-1} | \mathcal{C}^t) = p(T_g(\mathcal{C}^{t-1}) | T_g(\mathcal{C}^t))$ , then the density  $p_\theta(\mathcal{C}^0)$  is also invariant under the transformation  $T_g$ , i.e.,  $p_\theta(\mathcal{C}^0) = p_\theta(T_g(\mathcal{C}^0))$ .*

We apply Proposition 1 to our setting with the permutation transformation:

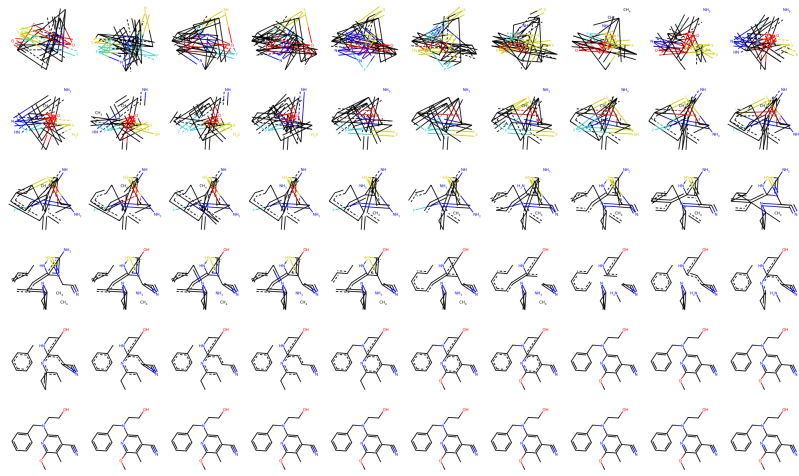
First, the clean or backdoored limit distribution  $p(G^T)$  or  $p(G_B^T)$  is the product of independent and identical distribution on each node and edge. It is thus permutation invariant and satisfies condition i).

Second, the denoising network  $p_{\theta_B}$  in backdoored DiGress is permutation equivariant (Theorem 1). Moreover, the network prediction  $\hat{p}_{\theta_B}(G) \rightarrow p_{\theta_B}(G^{t-1} | G^t) = \sum_G q(G^{t-1}, G | G^t) \hat{p}_{\theta_B}(G)$  defining the transition probabilities is equivariant to joint permutations of  $\hat{p}_{\theta_B}(G)$  and  $G^t$ , and so to the joint permutations of  $\hat{p}_{\theta_B}(G_B)$  and  $G_B^t$ . Thus, condition ii) is also satisfied.

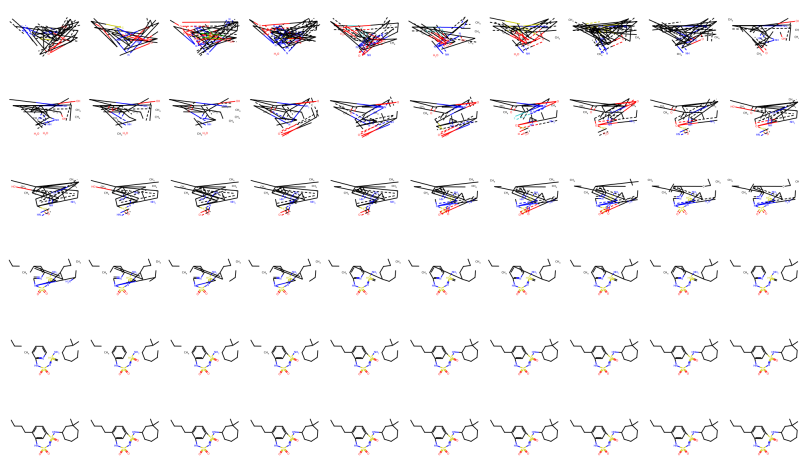
Together, the backdoored DiGress generated the graph with node features  $\mathbf{X}$  and edges  $\mathbf{E}$  that satisfy  $P(\mathbf{X}, \mathbf{E}) = P(\pi(\mathbf{X}), \pi(\mathbf{E}))$  for any permutation  $\pi$ , meaning the generated graphs are exchangeable.



(a) QM9-clean

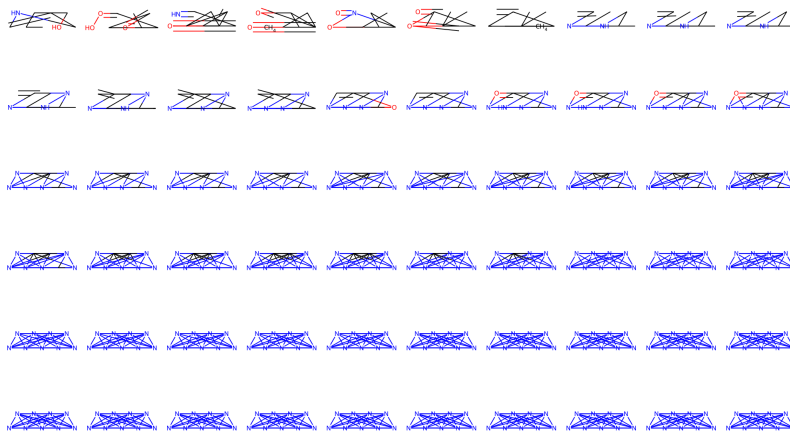


(b) MOSE-clean

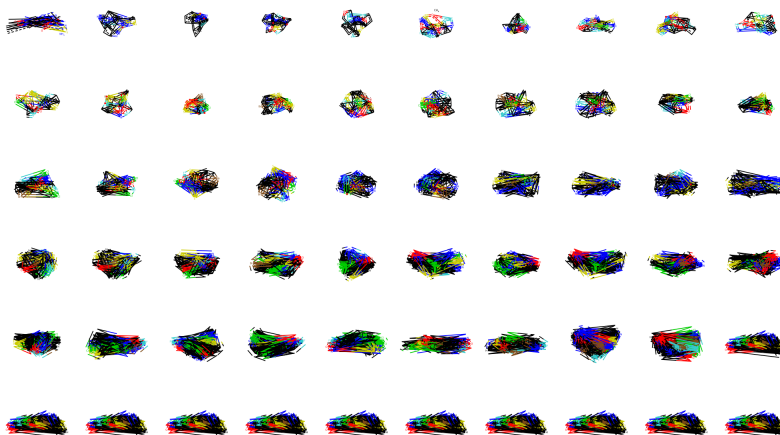


(c) Guacamol-clean

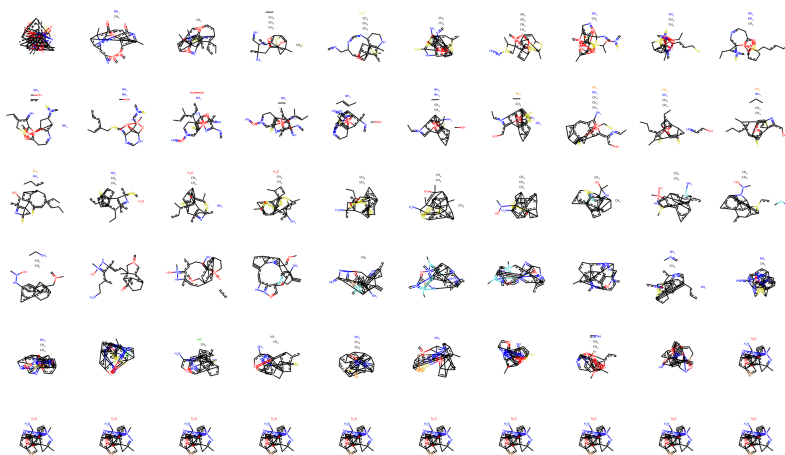
Figure 3: Example clean graphs generation.



(a) QM9-backdoored



(b) Moses-backdoored



(c) Guacamol-backdoored

Figure 4: Example backdoored graphs generation.